Taibah University

Journal of Taibah University Medical Sciences

www.sciencedirect.com

Original Article

Molecular docking-based virtual screening, drug-likeness, and pharmacokinetic profiling of some anti-*Salmonella typhimurium* cephalosporin derivatives

Philip John Ameji, M.Sc [a],[*], Adamu Uzairu, PhD [b], Gideon Adamu Shallangwa, PhD [b] and Sani Uba, PhD [b]

[a] *Department of Chemistry, Federal University Lokoja, Lokoja, Kogi State, Nigeria*
[b] *Department of Chemistry, Ahmadu Bello University, Zaria, Kaduna State, Nigeria*

المخلص

أهداف البحث: أدت حالات المقاومة المتزايدة للعلاجات بالمضادات الحيوية الموجودة في السلمونيلة التيفية الفأرية إلى جعل البحث عن أدوية جديدة مرشحة أمرا ضروريا. استخدمت الدراسة الحالية تقنية الالتحام الجزيئي لفحص مجموعة من نظائر السيفالوسبورين المضادة للبكتيريا ضد البروتين المرتبط بالبنسلين للبكتيريا. هذه هي المرة الأولى التي يتم فيها فحص نظائر السيفالوسبورين مقابل البروتين المضاد للبنسلين، وهو بروتين أساسي لتخليق ببتيدوغليكان من السلمونيلة التيفية الفأرية.

طرق البحث: تم استرجاع بعض مشتقات السيفالوسبورين من مستودع الأدوية. تم تحسين هياكل الجزيئات باستخدام الطريقة شبه التجريبية لبرنامج سبارتان ١٤ ومن ثم تم ربطها مع مواقع التفاعل النشطة لبروتين الربط بالبنسلين ١أ باستخدام برنامج أوتودوك فينا. تم اختيار أقوى الجزيئات المرتبطة كأكثر التركيبات الواعدة ومن ثم تم تقييم خصائص الامتصاص والتوزيع والأيض والطرد والسمية باستخدام خادم سويس أدمي عبر الإنترنت وبرنامج داتا ووريور للمعلومات الكيميائية. تم استخدام خادم كابسفلكس ٢.٠ لإجراء محاكاة الديناميكا الجزيئية على أكثر تركيب جزيئي-بروتين ثابت.

النتائج: تم اختيار المركبات ٣ و ٢٣ و ٢٨ بقيم تقارب الربط تبلغ على التوالي ٩,٢- كيلوكالوري/مول و ٨,٧- كيلوكالوري/مول و ٨,٩- كيلوكالوري/مول كأكثر التركيبات الواعدة. ترتبط الجزيئات المرتبطة بمواقع التفاعل النشطة لبروتين الربط بالبنسلين ١أ عن طريق التفاعلات الهيدروفوبية والترابط الهيدروجيني والتفاعلات الكهروستاتيكية. علاوة على ذلك، أظهرت تحليلات الامتصاص والتوزيع والأيض والطرد والسمية للجزيئات المرتبطة أنها تتمتع

بملفات دوائية جيدة وسمية مقبولة. بالإضافة إلى ذلك، أظهرت دراسة الديناميكا الجزيئية أن أكثر الجزيئات نشاطا ترتبط بشكل ملائم وديناميكي ببروتين الهدف.

الاستنتاجات: يمكن أن توفر نتائج هذا البحث منصة ممتازة نحو الاكتشاف والتصميم العقلاني للمضادات الحيوية الجديدة ضد السلمونيلة التيفية الفأرية. أيضا، يجب إجراء المزيد من الدراسات في الجسم الحي وفي المختبر على الأدوية المرشحة من أجل التحقق من نتائج هذا البحث.

الكلمات المفتاحية: السلمونيلة التيفية الفأرية؛ سيفالوسبورين؛ بروتين الربط بالبنسلين ١أ؛ بيتا-لاكتام؛ المضادات الحيوية

Abstract

Objective: The rising cases of resistance to existing antibiotic therapies in *Salmonella typhimurium* has made it necessary to search for novel drug candidates. The present study employed the molecular docking technique to screen a set of antibacterial cephalosporin analogues against penicillin-binding protein 1a (**PBP1a**) of the bacterium. This is the first study to screen cephalosporin analogues against **PBP1a**, a protein central to peptidoglycan synthesis in *S. typhimurium*.

Methods: Some cephalosporin analogues were retrieved from a drug repository. The structures of the molecules were optimized using the semi-empirical method of Spartan 14 software and were subsequently docked against the active sites of PBP1a using AutoDock vina software. The most potent ligands were chosen as the most promising leads and subsequently subjected to absorption, distribution, metabolism, excretion, and toxicity (ADMET) profiling using the SwissADME online server and DataWarrior chemoinformatics program. The CABSflex 2.0 server was used to carry out molecular

* Corresponding address: Department of Chemistry, Federal University Lokoja, P.M.B., 1154, Lokoja, Kogi State, Nigeria.
E-mail: ameji4real55@gmail.com (P.J. Ameji)
Peer review under responsibility of Taibah University.

ELSEVIER | **Production and hosting by Elsevier**

dynamics (MD) simulation on the most stable ligand −protein complex.

Results: Compounds 3, 23, and 28 with binding affinity (ΔG) values of −9.2, −8.7, and −8.9 kcal/mol, respectively, were selected as the most promising leads. The ligands bound to the active sites of PBP1a via hydrophobic bonds, hydrogen bonds, and electrostatic interactions. Furthermore, ADMET analyses of the ligands revealed that they exhibited sound pharmacokinetic and toxicity profiles. In addition, an MD study revealed that the most active ligand bound favorably and dynamically to the target protein.

Conclusion: The findings of this research could provide an excellent platform for the discovery and rational design of novel antibiotics against *S. typhimurium*. Additional *in vitro* and *in vivo* studies should be carried out on the drug candidates to validate the findings of this study.

Keywords: β-lactam; Antibiotics; Cephalosporin; PBP1a; *Salmonella typhimurium*

Introduction

Salmonella typhimurium is one of the *S. enterica* serovars responsible for non-typhoidal salmonellosis (NTS). The major clinical manifestations of this infection are abdominal cramp, diarrhea, and fever, which are life-threatening systemic illnesses that require urgent antibiotic therapy. Unlike typhoid fever whose prevalence is found in developing countries, NTS is a global infection. The annual morbidity and mortality rates of gastroenteritis, a common form of NTS, are estimated to be 93.8 million cases and 155,000 deaths, respectively.[1] In addition to gastroenteritis, *S. typhimurium* causes bacteremia and focal systemic infections, known as invasive non-typhoidal Salmonellosis (iNTS).[2,3] The annual incidence of iNTS in Sub-Saharan Africa was estimated to be 175−388 cases per 100,000 children and 2000−7500 cases per 100,000 human immunodeficiency virus (HIV)-infected adults with a death rate of 20−25% among infected persons.[4−9]

The major sources of transmission of this bacterium include contaminated animal-derived products, contact with infected persons and pets, and the consumption of fruits and vegetables associated with recent outbreaks.[10−13]

The startling statistics of morbidity and mortality associated with NTS and iNTS are further compounded by the emerging trend of multidrug-resistant strains of *S. typhimurium* against existing antibiotics, which are currently the only available treatment options.[14−16] Thus, a search for novel drug candidates with enhanced potencies than existing ones have become necessary. However, the discovery of new drugs has been impeded by the enormous resources and time it takes from the discovery stage, through the preclinical and clinical stages, to the formulation stage. Nonetheless, the application of computer-aided techniques, such as molecular docking-based virtual screening as well as pharmacokinetic and toxicity profiling, have helped mitigate the aforementioned challenges by preventing the trial and error methods that characterize traditional drug discovery techniques.[17−21]

The high failure of many drug candidates is attributable to poor pharmacokinetic and toxicity profiles, which account for more than of half of all failures in clinical trials. Thus, an integral part of virtual screening is to assess the drug-likeness of therapeutic ligands with respect to their absorption, distribution, metabolism, excretion, and toxicity (ADMET) parameters.[20−22]

Peptidoglycan is the major structural component of most bacterial cell walls and consists of glycan chains with repeating disaccharide N-acetylmuramic acid-β-1,4-N-acetylglucosamine (MurNAc-GlcNAc). Its dominant roles include the maintenance of cell shape and provision of mechanical strength to prevent osmotic rupture of the cell. The synthesis of this important biomolecule requires glycosyltransferase (GTase) and transpeptidase (Tpase) activities to polymerize and cross-link the glycan chains, respectively. Penicillin-binding protein 1a (PBP1a) is one of the most important peptidoglycan synthases in rod-shaped Gram-negative bacteria. In addition to having both GTase and TPase activities, PBP1a also helps bacteria survive in alkaline medium. These crucial roles of PBP1a in Gram-negative bacteria make it a good target for antibiotics.[23−26]

Cephalosporins are composed of a six-membered ring with a sulfur atom attached to a β-lactam ring. Similar to other β-lactam antibiotics, they function by inhibiting the last step in the synthesis of peptidoglycan by acylating the transpeptidase (PBP1a) involved in cross-linking peptides to form the biomolecule, resulting in activation of an autolytic system that eventually leads to cell death.[27]

In an effort to discover novel drug candidates against *S. typhimurium*, some computer-based studies targeting different enzymes of the bacterium have recently been carried out.[28−33] The aim of this study was to apply computer-aided techniques to search for highly potent and non-toxic cephalosporin-based drug candidates that can strongly inhibit PBP1a, a crucial penicillin-binding protein of *S. typhimurium*.

Materials and Methods

Data set

A set of cephalosporin derivatives (ligands) with inhibitory activities against *S. typhimurium* were retrieved from the PubChem database (https//pubchem.ncbi.nlm.nih.gov). The biological activity of the compounds is expressed as the minimum inhibitory concentration (MIC). The structure, PubChem compound identity number, and MIC values for each member of the data set are presented in Table 1.

Ligand preparation

The two-dimensional (2D) structures of the compounds were generated using ChemDraw ultra 12.0 and exported

into the Spartan'14 V1.1.0 software interface, where their 3D structures were generated and subsequently subjected to energy minimization using semi-empirical (parametric method 3) procedures. The optimized species were saved in Protein Data Bank (PDB) file format and further exported into the AutoDock Vina interface where they were further prepared and saved in PDBQT file format.[34]

Protein preparation

The 3D crystal structure of the target macromolecule (PBP1a) was downloaded in PDB file format (PDB Code; 2OQO) from the PDB at www.rcsb.org/pdb. It was exported into the Discover Studio software interface where attached water molecules, ligands, and other heteroatoms were removed. The prepared protein was further exported into the AutoDock Vina interface where missing atoms were checked and repaired, and Kollman's charges and polar hydrogens were added. It was subsequently saved in PDBQT file format.

Molecular docking calculations

Docking calculations were performed in the PyRx interface using the AutoDock Vina option. The grid box was centered at X = 37.6571, Y = 37.7482, and Z = 21.9987, with a grid dimension of 50.4384 Å × 45.8988 Å × 45.0019 Å, thereby enclosing both the active site residues and the binding sites. After a series of ligand–receptor runs, the results were evaluated by Vina. The resulting poses of the ligands were clustered based on their conformational overlaps, and their binding affinities were calculated. The best pose from each group was selected, and the ligands were ranked based on their binding affinity values. The ligands with the best binding affinity values were chosen as the most promising leads to be subjected to further *in silico* assessments. The interaction of the ligands with the active sites of the protein target was visualized with the aid of Discovery Studio Visualizer v16.1.0.15350. As a quality control measure, the 3D chemical structure of cefuroxime, a cephalosporin-based antibiotic currently used for the treatment of Gram-negative bacterial infections, was retrieved from the PubChem DrugBank database, optimized, and docked with the PBP1a target. The binding affinity of cefuroxime was compared with that of the most promising ligands (MPLs).[31,34,35]

Drug-likeness assessment of the most promising leads

Drug-likeness is the qualitative description of oral bioavailability of a therapeutic compound. This assessment is very important due to the fact that many drugs are administered via the oral route. This important parameter was evaluated for the most promising leads using the famous Lipinski's rule of five. According to this rule, for a therapeutic molecule to be orally bioavailable, it must not violate more than one of the following parameters: molecular weight (MW) $\leq$ 500, number of hydrogen bond donors $\leq$ 5, octanol/water partition coefficient (LogP) $\leq$ 5 and number of hydrogen bond acceptors (HBAs) $\leq$ 10.[36] The

aforementioned physicochemical properties of the selected most promising leads were calculated with the aid of the SwissADME (www.swissadme.ch/) online tool.

ADMET evaluation of the most promising leads

Early assessment of the fates of therapeutic compounds in the biological system plays a pivotal role in modern drug discovery and development as it aids with the removal of non-drug-like candidates from the pool of bioactive compounds. The fate of potential drug candidates is determined by their absorption (A), distribution (D), metabolism (M), excretion (E), and toxicity (T) in the biological system. ADMET evaluation of the selected bioactive compounds was performed with the aid of SwissADME (www.swissadme.ch/) online resource and Osiris DataWarrior V5.5.0 chemoinformatics program.[34]

Molecular dynamics simulation

The dynamics of protein structures influence their bio-activities. However, the investigation of protein flexibility via wet laboratory experiments is often an arduous or impossible task, necessitating *in silico* approaches. An economical computational approach to studying protein flexibility in a biological system is the usage of coarse-grained simulation models in conjunction with the reconstruction of predicted structures to all-atom representation.[37] In this study, molecular dynamics (MD) simulations of the complex of the best ligand (compound 3) with PBP1a (PDB Code: 2OQO) was performed using the CABSflex 2.0 server at http://biocomp.chem.uw.edu.pl/CABSflex2/job/746d8804a364dc5/. The PDB file of the complex was uploaded to the server via the "browse" option. CABS-flex applies a set of simulation parameters and distance restraints, as discussed by Jamroz et al.[38,39] These settings were adopted to provide the best likely convergence between CABS-flex simulations and the consensus picture of protein fluctuations in aqueous solution derived by all-atom MD simulations for globular proteins. The results of the MD simulations were recorded as the root-mean-square-fluctuation (RMSF) of the protein structure. RMSF is the time average of the root-mean-square-deviation computed using equation (1) as follows:

$$RMSF = \sqrt{< (x_i - < x_i >)^2}, \qquad (1)$$

where x_i is the coordinate of particle i, and $\langle x_i \rangle$ is the ensemble average position of i.

Results

MD-based virtual screening

The PBP1a of *S. typhimurium* (Figure 1) plays significant physiological and biochemical roles in the bacterium. Binding of bioactive ligands to the active sites of this macromolecule inhibits its ability to perform its primary

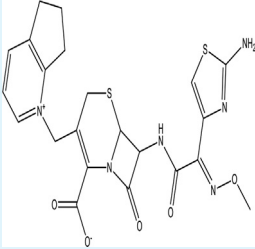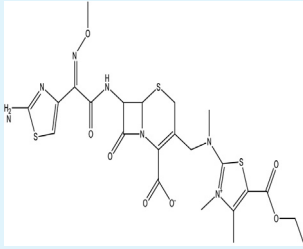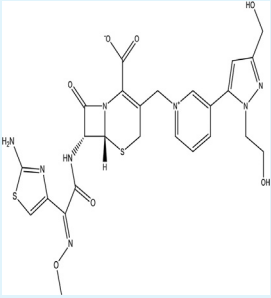**Table 1: Structure, PubChem compound identification, and biological activities of the data set.**
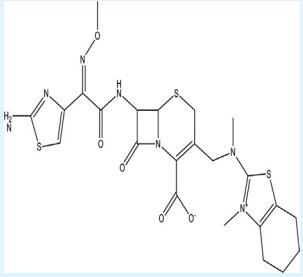
Compound No.	Structure	MIC (µg/mL)	Compound No.	Structure	MIC (µg/mL)
1	 13138129	1.60	17	 44269866	1.31
2	 118753875	0.41	18	 44269898	1.31
3	 118753876	1.01	19	 10460518	1.01
4	 118753877	0.71	20	 10054849	1.31
5	 118753879	0.71	21	 44269930	1.31

Table 1 (*continued*)

Compound No.	Structure	MIC (µg/mL)	Compound No.	Structure	MIC (µg/mL)
6	118753880	1.31	22	5479539	1.60
7	118753881	1.01	23	118753852	0.30
8	118753882	1.31	24	118753853	0.89
9	118753883	1.31	25	118753854	0.89

Table 1 (*continued*)

Compound No.	Structure	MIC (µg/mL)	Compound No.	Structure	MIC (µg/mL)
10	118753884	1.01	26	118753855	0.89
11	118753885	1.01	27	118753867	0.60
12	10054849	1.31	28	118753868	0.30
13	44269930	1.31	29	118753869	0.30

Table 1 (*continued*)

Compound No.	Structure	MIC (µg/mL)	Compound No.	Structure	MIC (µg/mL)
14	5479539	1.60	30	118753870	0.30
15	44269851	1.01	R*		
16	44269853	1.31			

MIC: Minimum inhibitory concentration; R* = Reference antibiotic (cefuroxime).

function of participating in peptidoglycan synthesis in *S. typhimurium*, impairing the survival of the organism in the harsh extracellular milieu of the host cell. The results of the screening of the investigated cephalosporin derivatives (ligands) against the active sites of this target enzyme (PBP1a) are presented in Table 2. The strength of the binding interactions between the ligands and target macromolecule is expressed as change in Gibb's free energy of binding (ΔG). Increased negative value of ΔG connotes a higher binding affinity, and vice versa. However, ligands 3, 23, and 28 were selected as the MPLs because of their exceptional ΔG values of −9.2, −8.7, and −8.9 kcal/mol, respectively. The selected MPLs were found to be more potent when compared with the reference antibiotic
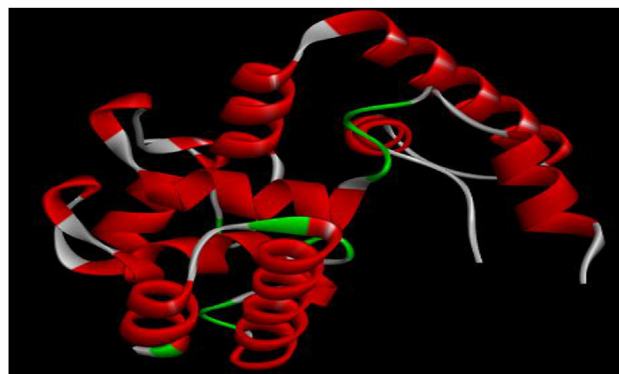
Figure 1: 3D structure of PBP 1a target.

Table 2: Binding affinity values of the data set of cephalosporin derivatives.

Compound No.	ΔG (kcal/mol)	S/n	ΔG (kcal/mol)	Compound No.	ΔG (kcal/mol)
1	−7.6	12	−8.0	23	−8.7
2	−7.9	13	−7.8	24	−8.5
3	−9.2	14	−8.4	25	−8.1
4	−8.1	15	−8.0	26	−7.9
5	−7.5	16	−8.1	27	−6.7
6	−8.6	17	−8.1	28	−8.9
7	−7.7	18	−8.6	29	−8.3
8	−8.0	19	−7.8	30	−8.5
9	−8.5	20	−7.7	R	−7.7
10	−8.6	21	−7.8		
11	−8.5	22	−8.4		

ligand 3 in complex with PBP 1a
(ΔG = -9.2 kcal/mol)

ligand 23 in complex with PBP 1a
(ΔG = -8.7 kcal/mol)

ligand 28 in complex with PBP 1a
(ΔG = -8.9 kcal/mol)

R in complex with PBP 1a
(ΔG = -7.7 kcal/mol)

Figure 2: 2D diagram of interraction of the most promisisng leads and R with the active sites of PBP 1a macromolecule.

Table 3: IUPAC nomenclatures of the MPLs and the major amino acid residues of PBP1a that they interact with.

Compound No.	IUPAC nomenclature	Major interacting amino acids	Number of H-bonds
3	(6R,7R)-7-((E)-2-(2-aminothiazol-4-yl)-2-(methoxyimino)acetamido)-3-((3-(5-(hydroxymethyl)-1H-pyrazol-3-yl)pyridin-1-ium-1-yl)methyl)-8-oxo-5-thia-1-azabicyclo[4.2.0]oct-2-ene-2-carboxylate	ALA81, ARG100, ARG225, LYS201, GLN121, ARG85	4
23	(E)-3-(((4-amino-1-methyl-5-phenylpyrimidin-1-ium-2-yl)thio)methyl)-7-(2-(2-aminothiazol-5-yl)-2-(((2-carboxypropan-2-yl)oxy)imino)acetamido)-8-oxo-5-thia-1-azabicyclo[4.2.0]oct-2-ene-2-carboxylate	GLU140, LYS137, GLN121, SER116, LYS124, ALA97, ARG85	7
28	(E)-7-(2-(2-aminothiazol-5-yl)-2-(((2-carboxypropan-2-yl)oxy)imino)acetamido)-3-(((1-methyl-7-morpholino-1H-[1,2,4]triazolo[1,5-c]pyrimidin-4-ium-5-yl)thio)methyl)-8-oxo-5-thia-1-azabicyclo[4.2.0]oct-2-ene-2-carboxylate	GLU83, GLY114, SER116, GLN121, LYS124, ASN125,	6
R	(Z)-3-((carbamoyloxy)methyl)-7-(2-(furan-2-yl)-2-(methoxyimino)acetamido)-8-oxo-5-thia-1-azabicyclo[4.2.0]oct-2-ene-2-carboxylic acid	ARG225, ARG85, GLN121, GLU83, SER116	4

MPLs: Most promising ligands; PBP1a: Penicillin-binding protein 1a.

Table 4: Drug-likeness profiles of the MPLs and cefuroxime.

Compound No.	3	23	28	Cefuroxime
Lipinski's Rule	yes	no	no	yes
HBA	9	10	12	9
HBD	4	4	3	3
MW (g mol^{-1})	570.6	684.8	718.8	424.4
cLogP$_{(o/w)}$	−1.33	−0.07	−1.13	−0.33

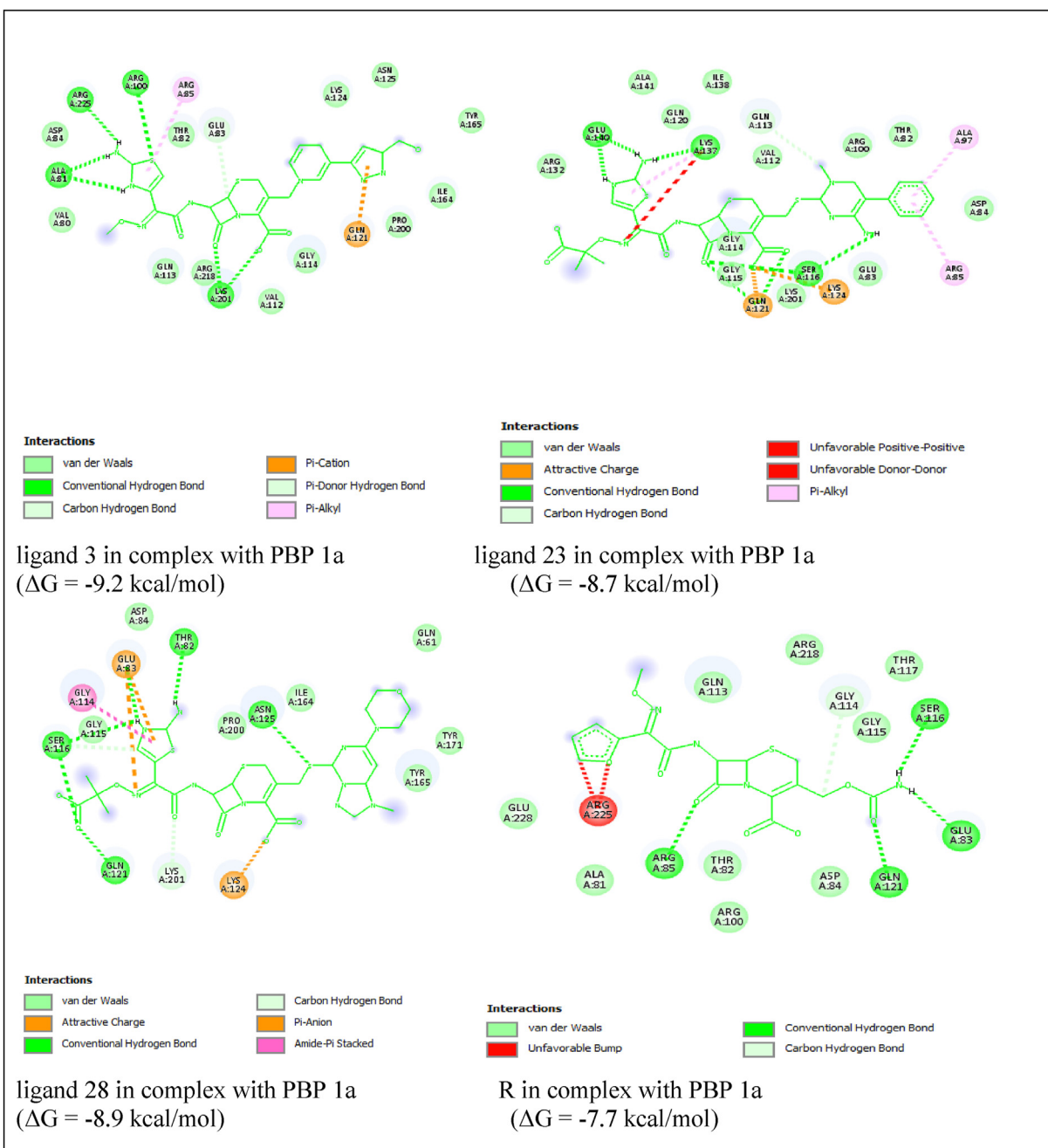HBA: Hydrogen bond acceptor; HBD: Hydrogen bond donor; MPLs: Most promising ligands; MW: Molecular weight.

(cefuroxime), which binds to the protein target with ΔG of −7.7 kcal/mol.

Modes of interaction of the MPLs with PBP1a

Figure 2 presents the 2D diagram of interaction of the MPLs and cefuroxime with the active sites of the PBP1a target. The major amino acid residues of the macromolecule that interacts with the ligands are presented in Table 3.

Table 5: ADMET profiles of the most promising ligands and cefuroxime.

Compound No.	Toxicity endpoints	Pharmacokinetic	Oral bioavailability score
3	Mutagenic: **None** Tumorigenic: **None** Reproductive effect: **None** Irritant: **None**	CYP450 inhibitor: No P-gp substrate: No GIA: Yes BBB Permeation: No	0.17
23	Mutagenic: **None** Tumorigenic: **None** Reproductive effect: **None** Irritant: **None**	CYP450 Inhibitor: No P-gp substrate: No GIA: Yes BBB: No	0.11
28	Mutagenic: **None** Tumorigenic: **None** Reproductive effect: **None** Irritant: **None**	CYP450 inhibitor: No P-gp substrate: Yes GIA: Yes BBB: No	0.11
R	Mutagenic: **Yes** Tumorigenic: **None** Reproductive effect: **None** Irritant: **None**	CYP450 inhibitor: No P-gp substrate: No GIA: Yes BBB Permeation: No	0.11

ADMET: Absorption, distribution, metabolism, excretion, and toxicity; BBB: Blood−brain barrier, CYP450: Cytochrome P450; GIA: Gastrointestinal absorption P-gp: P-glycoprotein.

a

b
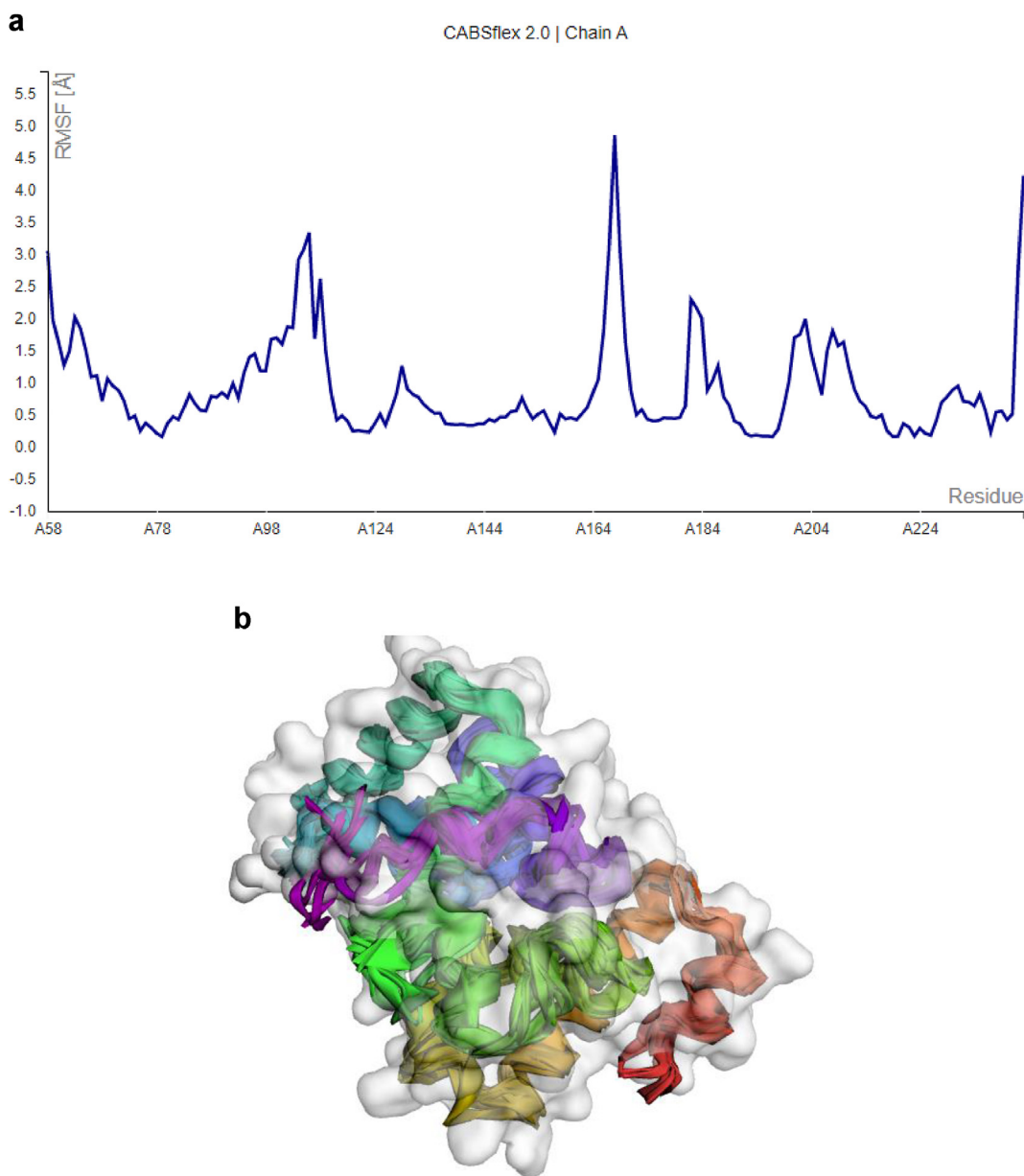
Figure 3: a: Fluctuation plot of PBP 1a. **b**: Model-all diagram of PBP 1a. **c**: Contact map of the residues of PBP 1a.

Oral bioavailability evaluation and ADMET profiles of the MPLs

Oral bioavailability (drug-likeliness) is a function of certain physicochemical properties of a molecule. These properties were computed for the MPLs and cefuroxime, and the results are presented in Table 4. Also, the pharmacokinetic and toxicity profiles of the ligands are presented in Table 5.

MD study

Figure 3a presents the fluctuation plot of the simulation, whereas Figure 3b and c give the model-all diagram and residue contact map, respectively.

c
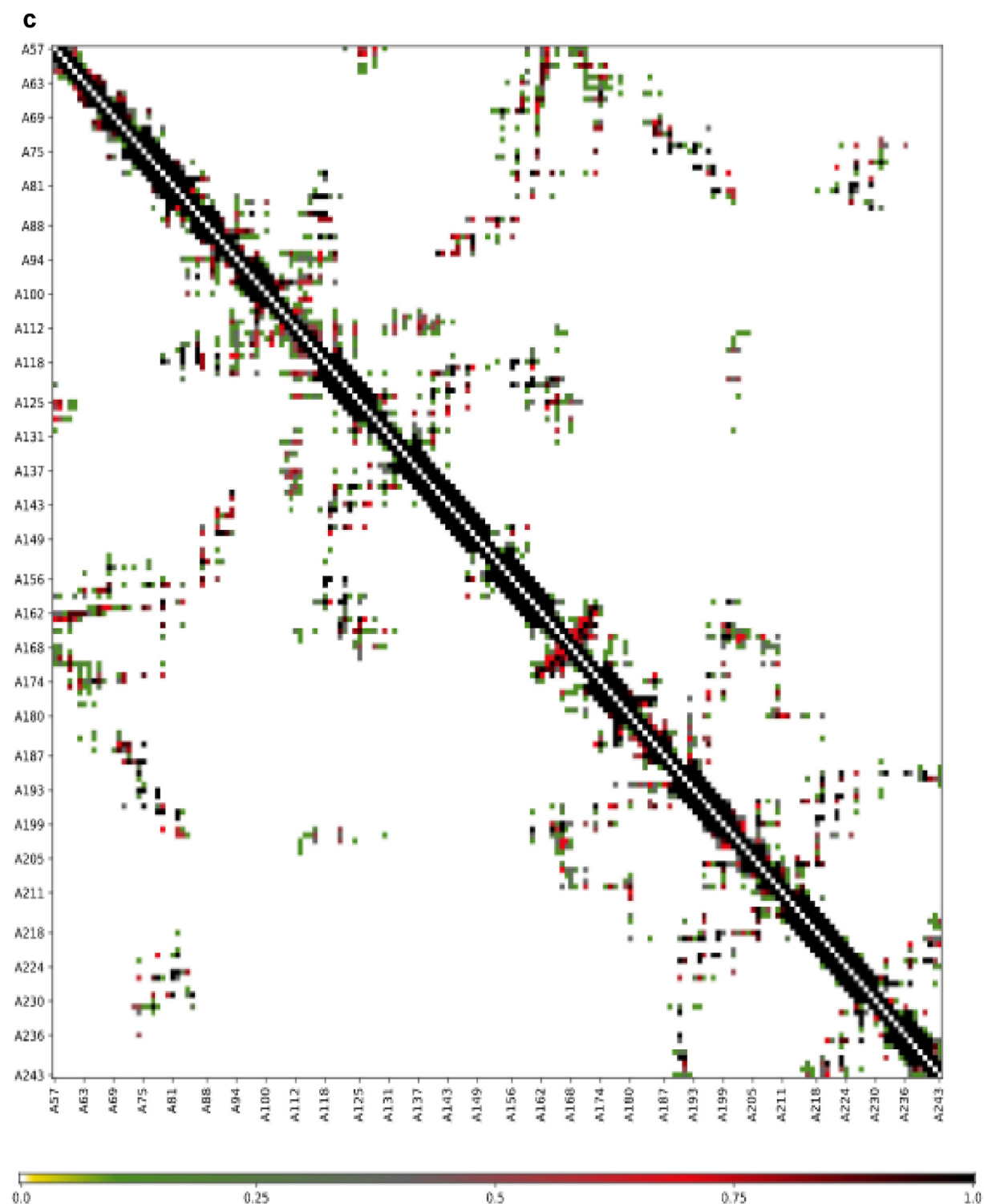
Figure 3: (*continued*).

Discussion

All β-lactam-based antibiotics (cephalosporin inclusive) function by antagonizing the PBP of bacteria with the resultant effect of obstructed cell wall synthesis in the organisms leading to their inactivation or death. The results of molecular docking-based virtual screening of the studied ligands against PBP1a, a PBP of *S. typhimurium*, (Table 2) revealed that the ligands bound excellently to the active sites of the target with binding affinity values ranging from −6.7 to −9.2 kcal/mol. Compounds 3, 23, and 28 with ΔG values of −9.2, −8.7, and −8.9 kcal/mol, respectively, were selected as the MPLs because of their excellent potencies against the PBP1a target. These ΔG

values of the MPLs were higher than that of cefuroxime ($\Delta G = -7.7$ kcal/mol), an approved β-lactam antibiotic for the treatment of *S. typhimurium*-induced salmonellosis, indicating that the MPLs could be more potent than standard drugs. This finding is similar to that of Jasmine et al.,[33] who performed molecular docking calculations on D-benzylpenicilloic acid against β-lactamase of human *S. typhimurium*. The authors reported that the ligand binds better than standard inhibitors of the β-lactamase target.

Table 3 presents the IUPAC nomenclatures and amino acid side chains of the PBP1a target with which the selected ligands interact with. Assessment of the 2D diagram of interactions with the active sites of the target macromolecule (Figure 2) revealed that compound 3 bound to the active sites of the target protein via the formation of six conventional hydrogen bonds with Ala-81, Arg-100, Arg-225, and Lys-201 amino acid residues. Additionally, the ligand formed a pi–cation interaction with Gln-121 and a pi–alkyl interaction with Arg-85 amino acid residues. It is pertinent to note that hydrophobic, electrostatic, and hydrogen bond interactions were found in the complex of ligand 3 with the PBP1a of *S. typhimurium*. Also, ligand 23 with a binding affinity of −8.7 kcal/mol against the target macromolecule displayed the following interactions with the amino acid residues of the protease: attractive charge associations with Gln-121 and Lys-124; unfavorable donor–donor interactions with Lys-137; and pi–alkyl interactions with Lys-137, Ala-97, and Arg-85. These interactions were stabilized by the formation of conventional hydrogen bonds with Ser-116, Gln-121, Lys-137, and Glu-140. Again, hydrophobic, electrostatic, and hydrogen bond interactions were found in the ligand/protein complex. Furthermore, ligand 28 formed a complex with the active sites of PBP1a with a binding affinity of −8.9 kcal/mol. The interactions found in this complex were: attractive charge interaction with Glu-83; two pi–anion interactions with Lys-124; an amide pi-stacked interaction with Gly-114; and six conventional hydrogen bonds with Asn-125, Thr-82, Glu-83, Ser-116, and Gln-121. Similar to ligands 3 and 23, hydrophobic, electrostatic, and hydrogen bond interactions were also found in the complex of ligand 28 with PBP1a. This could be responsible for their exceptional potencies against the target macromolecule. In addition, the standard ligand, cefuroxime, bound to PBP1a with a ΔG of −7.7 kcal/mol. The following interactions were found between the ligand and the active sites of the protein target: an unfavorable bond with Arg-225 and four conventional hydrogen bonds with Arg-85, Gln-121, Glu-83, and Ser-116.

By interacting with the active sites of the protein target via conventional hydrogen bonds with Gln-121, Ser-116, and Glu-83, ligand 28 bound with PBP1a in a mechanism similar to the standard ligand (R). Ligand 23 displayed a similar mode of interaction with R via conventional hydrogen bonds with Ser-116 and Gln-121 amino acid residues of the target macromolecule. Ligand 3 with the best potency bound to the target sites of the macromolecule via a mechanism entirely different from cefuroxime.

Drug-likeness assessment is a measure of oral bioavailability of a therapeutic molecule. It is defined as the extent and rate at which an orally administered drug enters the systemic circulation and reaches the target sites.[40] The Lipinski's rule of five was used to filter the MPLs for their drug-likeness. Table 4 presents the outcome of the bioavailability screening of the MPLs. Compound 3 like cefuroxime, passed the test and as such could be considered orally bioavailable. Ligands 23 and 28 by having an MW > 500 and HBA > 10, violated two of the indices and as such may not possess excellent oral absorption according to Lipinski's rule of five.[41] However, if compounds 23 and 28 are to be used as templates for drug discovery due to their excellent potencies, their structures should be modified for enhanced oral bioavailability.

Pharmacokinetic deals with fate of a therapeutic compound in the biological system with particular reference to its absorption (A), distribution (D), metabolism (M), and excretion (E). The ADME and toxicity (T) profiles of the MPLs are presented in Table 5. Poor ADMET profiles account for the high attrition rates of drug candidates in the clinical stage of drug development. Hence, the profiling of drug candidates prior to clinical stage is a rational and cost effective drug discovery strategy. All ligands, such as cefuroxime, were found to possess gastrointestinal absorption potential.

Also, the blood–brain barrier (BBB) refers to a microvascular endothelial cell layer of the brain that separates the brain from blood circulation, thereby preventing entry of toxins into the central nervous system (CNS).[42,43] The BBB permeation data displayed in Table 5 for the MPLs and cefuroxime revealed that all ligands, such as cefuroxime, do are not able to penetrate the BBB. This could be advantageous considering the fact that they may not have any deleterious effects on the CNS when used as drugs. Penetration of the BBB may only be mandatory for compounds targeting the CNS.[44]

P-glycoproteins (P-gps) are membrane transporters that limit the cellular uptake of its substrates from blood circulation into the brain via its efflux action.[45,46] Ligands 3 and 23, similar to cefuroxime, were found to be non-substrates of P-gps (Table 5) and as such may be unaffected by the efflux action of P-gp. Conversely, ligand 28, which happens to be substrate of the proteins, may have its serum concentrations grossly reduced leading to therapeutic failure if used as drug except if co-administered with inhibitors of P-gps.

Oral bioavailability is concerned with the fraction of the active form of a therapeutic compound that reaches the systemic circulation unchanged. Drugs with an oral bioavailability score >0.1 are considered orally bioavailable.[47,48] The bioavailability scores of the MPLs and cefuroxime (Table 5) were found to range from 0.11 to 0.17, indicating their good oral bioavailability. However, ligand 3 with a score of 0.17 displayed the best oral bioavailability in line with the prediction of Lipinski's rule of five.

Evaluation of the metabolism and biotransformation of drug candidates is one of the crucial stages in modern drug discovery. This important role is performed by the cytochrome P450 (CYP450) monooxygenase family. Inhibition of CYP450 enzymes by a therapeutic compound could lead to poor bioavailability and toxicity profiles due to bioaccumulation.[49] The metabolism of the MPLs and cefuroxime were performed against five isoforms of CYP450, namely CYP1A2, CYP2C19, CYP2C9, CYP2D6,

and CYP3A4. The results presented in Table 5 showed that none of the ligands was an absolute inhibitor of CYP450 enzymes. This indicates that they have a high chances of being metabolized, biotransformed, and excreted from the biological system. Also, the toxicity of the ligands evaluated using mutagenicity, tumorigenic effect, reproductive effect, and irritating effect as endpoints revealed that all of the MPLs possessed none of the aforementioned tendencies and as such may not pose a significant toxicity threat.

To determine the stability of the interaction of ligand 3 with the target protein, the protein−ligand complex was subjected to MD simulation study. The results of the MD study presented as a plot of RMSF against the protein residues of PBP1a (Figure 3a) revealed that most of the active residues of the target macromolecule fluctuated stably around less than 2.0 Å, an indication that the protein structure is stable and does not diverge significantly from its initial structure. The significant divergence observed for residues A112 (3.3 Å), A168 (4.8 Å), and A246 (4.2 Å) could be the result of some structural changes that the protein undergoes. Also, the 3D structures of the 10 final models are presented in the "model-all" set (Figure 3b). The different visuals in the model attests to the structural heterogeneity of the macromolecule. Additionally, the detailed view of the residue−residue interaction pattern of the protein is presented by the "contact map" in Figure 3c. The interaction within a pair of residues is denoted by each dot in the map, and the frequency of occurrence of these interactions is dependent on the color of the map. The prevalence of deep dark colors on a scale of 1.0 (Figure 3c) indicates that strong residue−residue interactions abound among the residues of the PBP1a protein target.

Conclusion

The search for novel drug candidates for the treatment of *S. typhimurium*-induced salmonellosis is a continuum considering the rising cases of resistance to existing antibiotics by this pathogenic microbe. In this study, the molecular docking technique was used to virtually screen a set of bioactive cephalosporin derivatives against the PBP of the bacterium. Three highly potent drug candidates were filtered out as the most promising leads. *In silico* ADMET analysis carried out on the selected ligands revealed that they exhibited positive pharmacokinetic and toxicity profiles. MD simulation of the most stable complex revealed that the ligand (compound 3) bound favorably to the target protein (PBP1a) in a dynamic manner. The findings of this research could provide excellent leverage towards the discovery and rational design of novel antibiotics that could arrest the deleterious effect of multidrug drug resistance in *S. typhimurium*.

Source of funding

Conflict of interest

The authors have no conflict of interest to declare.

Ethical approval

Not applicable.

Authors' contributions

The research was designed by AU, and supervised by AGS and SU. PJA carried out the computational analyses and drafted the manuscript. All authors have critically reviewed and approved the final draft and are responsible for the content and similarity index of the manuscript.

Acknowledgments

References

1. Majowicz SE, Musto J, Scallan E, Angulo FJ, Kirk M, O'Brien SJ, et al., International Collaboration on Enteric Disease "Burden of Illness" Studies. The global burden of non typhoidal *Salmonella* gastroenteritis. **Clin Infect Dis Off Publ Infect Dis Soc Am 2010**; 50: 882−889. https://doi.org/10.1086/650733.

2. Mandal BK, Brennand J. Bacteremia in Salmonellosis; a 15 year retrospective study from regional infectious diseases unit. **Br Med J 1998**; 297: 1242−1243.

3. Marzel A, Desai PT, Nissan I, Schorr YI, Suez J, Valinsky L, et al. Integrative analysis of salmonellosis in Israel,1995−2012 reveals association of serovar 9,12:l,v: with extra intestinal infections, dissemination of endemic *S*. Typhimurium DT104 bio types and a severe under-reporting of outbreaks. **J Clin Microbiol 2014**; 52: 2078−2088.

4. Crump JA, Medalla FM, Joyce KW, Krueger AL, Hoekstra RM, Whichard JM, et al. Antimicrobial resistance among invasive nontyphoidal *Salmonella enterica* isolates in the United States: national antimicrobial resistance monitoring system, 1996 to 2007. **Antimicrob Agents Chemother 2011**; 55: 1148−1154.

5. Feasey NA, Dougan G, Kingsley RA, Heyderman RS, Gordon MA. Invasive non-typhoidal salmonella diseases: an emerging and neglected tropical diseases in Africa. **Lancet 2012**; 379: 2489−2499. https://doi.org/10.1016/S0140-6736(11)61752-2.

6. Helms M, Ethelberg S, Molbak K. International *Salmonella* Typhimurium DT104 infections, 1992−2001. **Emerg Infect Dis 2005**; 11: 859−867.

7. Maclennan CA. Out of Africa: links between invasive nontyphoidal disease, typhoid fever and malaria. **Clin Infect Dis Off Publ Infect Dis Soc Am 2014**; 58: 648−650. https://doi.org/10.1093/cid/cit803.

8. Meakins S, Fisher IS, Berghold C, Gerner-Smidt P, Tschape H, Cormican M, et al. Antimicrobial drug resistance in human nontyphoidal *Salmonella* isolates in Europe 2000−2004: a report from the Enter-net International Surveillance Network. **Microb Drug Resist 2008**; 14: 31−35.

9. Ohad G, Erin CB, Guntram AG. Same species, different diseases: how and why typhoidal and non-typhoidal *Salmonella enterica* serovars differ. **Front Microbiol 2014**; 5(391): 1−10. https://doi.org/10.3389/fmicb.2014.00391.

10. Haeusler GM, Curtis N. Non-typhoidal salmonella in children: microbiology, epidemiology and treatment. **Adv Exp Med Biol 2013**; 764: 13−26. https://doi.org/10.1007/978-1-4614-4726-92.

11. Jackson BR, Griffin PM, Cole D, Walsh KA, Chai SJ. Outbreak associated with Salmonella enterica serotypes and food commodities, United States, 1998-2008. **Emerg Infect Dis 2013**; 19: 1239−1244. https://doi.org/10.3201/eid1908.121511.

12. Rahman HS, Mahmoud BM, Othman HH, Amin K. A review of history, definition, classification, source, transmission, and pathogenesis of Salmonella: a model for human infection. **J Zankoy Sulaimani Part A 2018**; 20: 11−20.

13. Sharifa EWP, Netty D, Sangaran G. Paper review of factors, surveillance and burden of food borne disease outbreak in Malaysia. **Malays J Public Health Med 2013**; 13: 98−105.

14. Brunelle BW, Bearson BL, Bearson SMD, Casey TA. Multidrug-resistant *Salmonella enterica* serovar Typhimurium isolates are resistant to antibiotics that influence their swimming and swarming motility. **mSphere 2017**; 2:e00306-17. https://doi.org/10.1128/mSphere.00306-17.

15. Overton JM, Linke L, Magnuson R, Broeckling CD, Rao S. Metabolomic profiles of multidrug-resistant Salmonella Typhimurium from humans, bovine, and porcine hosts. **Animals 2022**; 12: 1518. https://doi.org/10.3390/ani12121518.

16. Pławińska-Czarnak J, Wódz K, Kizerwetter-Swida M, Bogdan J, Kwieciński P, Nowak T, et al. Multi-drug resistance to *Salmonella* spp. when isolated from raw meat products. **Antibiotics 2022**; 11: 876. 10.3390/.

17. Macalino SJY, Gosu V, Hong S, Choi S. Role of computer-aided drug design in modern drug discovery. **Arch Pharm Res 2015**; 38: 1686−1701. https://doi.org/10.1007/s12272-015-0640-5.

18. Chen C, Wang T, Wu F, Huang W, He G, Ouyang L, et al. Combining structure-based pharmacophore modeling, virtual screening, and in silico ADMET analysis to discover novel tetrahydro-quinoline based pyruvate kinase isozyme M2 activators with antitumor activity. **Drug Des Devel Ther 2014**; 8: 1195−1210.

19. Vardhan S, Sahoo SK. In silico ADMET and molecular docking study on searching potential inhibitors from limonoids and triterpenoids for COVID-19. **Comput Biol Med 2020**; 124: 103936.

20. Opo FADM, Rahman MM, Ahammad F, Ahmed I, Bhuiyan MA, Asiri AM. Structure-based pharmacophore modeling, virtual screening, molecular docking and ADMET approaches for identification of natural anticancer agents targeting XIAP protein. **Sci Rep 2021**; 11: 4049.

21. Vlasiou MC, Petrou CC, Sarigiannis Y, Pafiti KS. Density functional theory studies and molecular docking on xanthohumol, 8-prenylnaringenin and their symmetric substitute diethanolamine derivatives as inhibitors for colon cancer-related proteins. **Symmetry 2021**; 13: 948.

22. Daina A, Michielin O, Zoete V. SwissADME: a free web tool to evaluate pharmacokinetics, drug-likeness and medicinal chemistry friendliness of small molecules. **Sci Rep 2017**; 7: 42717.

23. Mueller AE, Egan JFA, Breukink E, Vollmer W, Levin AP. Plasticity of *E. coli* cell wall metabolism promotes fitness and antibiotic resistance across environmental conditions. **Elife 2019**; 8:e40754. https://doi.org/10.7554/eLife.40754.

24. Typas A, Banzhaf M, Gross CA, Vollmer W. From the regulation of peptidoglycan synthesis to bacterial growth and morphology. **Nat Rev Microbiol 2012**; 10: 1−10.

25. Vollmer W, Blanot D, De Pedro MA. Peptidoglycan structure and architecture. **FEMS Microbiol Rev 2008**; 32: 149−167.

26. Yin J, Zhang T, Cai J, Lou J, Cheng D, Zhouet W, et al. PBP1a glycosyltransferase and transpepdidase activities are both required for maintaining cell morphology and envelope integrity in *Shewanella oneidensis*. **FEMS Microbiol Lett 2020**; 367(3). https://doi.org/10.1093/femsle/fnaa026.

27. Leone S, Damiani G, Pezone I, Kelly ME, Cascella M, Alfieri A, et al. New antimicrobial options for the management of complicated intra-abdominal infections. **Eur J Clin Microbiol Infect Dis 2019**; 38(5): 819−827.

28. Abishad P, Niveditha P, Unni V, Vergis J, Kurkure NV, Chaudhari S, et al. In silico molecular docking and in vitro antimicrobial efficacy of phytochemicals against multi-drug-resistant enteroaggregative *Escherichia coli* and non-typhoidal *Salmonella* spp. **Gut Pathog 2021**; 13: 46. https://doi.org/10.1186/s13099-021-00443-3.

29. Almeida FA, Pinto UM, Vanetti MCD. Novel insights from molecular docking of SdiA from *Salmonella* Enteritidis and *Escherichia coli* with quorum sensing and quorum quenching molecules. **Microb Pathog 2016**; 99: 178e190.

30. Durhan B, Yalçın E, Çavuşoğlu K, Acar A. Molecular docking assisted biological functions and phytochemical screening of *Amaranthus lividus* L. extract. **Sci Rep 2022**; 12: 4308. https://doi.org/10.1038/s41598-022-08421-8.

31. Nagasinduja V, Shahitha S, Prakash B, Kumar DJ. Molecular docking analysis of beta-lactamase from *Salmonella* species with eicosane. **Bioinformation 2022**; 18(8): 669−674.

32. Gnanendra S, Mohamed S, Natarajan J. Identification of potent inhibitors for *Salmonella typhimurium* quorum sensing *via* virtual screening and pharmacophore modeling. **Comb Chem High Throughput Screen 2013**; 6(10): 1−14.

33. Jasmine SKMd, Vidya SRG, Gorityala N, Sagurthi SR, Mungapati S, Manikanta KN, et al. In silico modeling and docking analysis of CTX-M-5, cefotaxime-hydrolyzing β-lactamase from human-associated *Salmonella* Typhimurium. **J Pharmacol Pharmacother 2022**; 1−13.

34. Ameji JP, Uzairu U, Shallangwa GA, Uba S. Virtual screening of novel pyridine derivatives as effective inhibitors of DNA gyrase (GyrA) of *Salmonella typhi*. **Curr Chem Lett 2022**; 12: 1−16.

35. Lewis RA, Wood D. Modern 2D QSAR for drug discovery. **Wiley Interdiscip Rev Comput Mol Sci 2014**; 4: 505−522.

36. Lipinski CA. Lead and drug-likeness compounds: the rule of five revolution. **Drug Discov Today Technol 2004**; 1(4): 337−341. https://doi.org/10.1016/j.ddtec.2004.

37. Kuriata A, Gierut AM, Oleniecki T, Ciemny MP, Kolinski A, Kurcinski M, et al. CABS-flex 2.0: a web server for fast simulations of flexibility of protein structures. **Nucleic Acids Res 2018**; 46: 339−343. https://doi.org/10.1093/nar/gky356.

38. Jamroz M, Orozco M, Kolinski A, Kmiecik S. Consistent view of protein fluctuations from all-atom molecular dynamics and coarse-grained dynamics with knowledge-based force-field. **J Chem Theory Comput 2013**; 9: 119−125.

39. Jamroz M, Kolinski A, Kmiecik S. CABS-flex predictions of protein flexibility compared with NMR ensembles. **Bioinformatics 2014**; 30: 2150−2154.

40. El-Kattan A, Varma M. Oral absorption, intestinal metabolism and human oral bioavailability. In: *Topics on Drug Metabolism*10; 2012, 31087.

41. Paramashivam SK, Elayaperumal K, Natarajan B, Devi Ramamoorthy M, Balasubramanian S, Dhiraviam KN. *In silico* pharmacokinetic and molecular docking studies of small molecules derived from *Indigofera aspalathoides* Vahl targeting receptor tyrosine kinases. **Bioinformation 2015**; 11: 73.

42. Konig F, Muller F. Transporters and drug-drug interactions: important determinants of drug disposition and effects. **Pharmacol Rev 2013**; 65: 944−966.

43. Wang Y, Xing J, Xu Y, Zhou N, Peng J, Xiong Z, et al. In silico ADME/T modelling for rational drug design. **Q Rev Biophys 2015**; 48: 488−515.

44. Borra NK, Kuna Y. Evolution of toxic properties of anti Alzheimer's drugs through Lipinski's rule of five. **Int J Pure Appl Biosci 2013**; 1: 28–36.

45. Levin GM. P-glycoprotein: why this drug transporter may be clinically important. **Curr Psychiatry 2012**; 11: 38–40.

46. Lin JH, Yamazaki M. Role of P-glycoprotein in pharmacokinetics: clinical implications. **Clin Pharmacokinet 2003**; 42(1): 59–98. https://doi.org/10.2165/00003088-200342010-00003.

47. Martin YC. A bioavailability score. **J Med Chem 2005**; 48(9): 3164–3170. https://doi.org/10.1021/jm0492002.

48. Olivares-Morales A, Hatley OJ, Turner D, Galetin A, Aarons L, Rostami-Hodjegan A. The use of ROC analysis for the qualitative prediction of human oral bioavailability from animal data. **Pharm Res 2014**; 31(3): 720–730.

49. Chow HS, Garland LL, Hsu CH, Vining DR, Chew WM, Miller JA, et al. Resveratrol modulates drug-and carcinogen metabolizing enzymes in a healthy volunteer study. **Cancer Prev Res 2010**; 3: 1168–1175.